of the absolute percentage errors. Such minimization results in the following correlation constants:

$$a = 0.83, \qquad a_1 = 0.03, \qquad a_2 = 0.78$$

$$b_1 = 0.58, \qquad b_2 = 1.38$$

The average absolute percentage error that corresponds to these constants is 4.2%. The error bounds on the experimental determination of x_T are ∓ 0.08. A comparison of the variation in the correlated and actual values of x_T with $1/\Gamma_1^2\Gamma_2^2$ is shown in Fig. 1.

Conclusion

The correlation presented here can be used to estimate the transition onset location in low-speed flow over a long swept cylinder for different sweep angles and freestream Reynolds numbers.

References

[1]Poll, D. I. A., "Some Observations of the Transition Process on the Wind-Ward Face of a Long Yawed Cylinder," *Journal of Fluid Mechanics*, Vol. 150, 1985, pp. 329–356.

[2]Masad, J. A., and Malik, M. R., "Effects of Body Curvature and Nonparallelism on the Stability of Flow over a Swept Cylinder," *Physics of Fluids*, Vol. 6, No. 7, 1994, pp. 2363–2379.

Simulation of Three-Dimensional Symmetric and Asymmetric Instabilities in Attachment-Line Boundary Layers

Ronald D. Joslin*
NASA Langley Research Center, Hampton, Virginia 23681-0001

Introduction

ON a swept wing, contamination along the leading edge, Tollmien–Schlichting waves, stationary or traveling crossflow vortices, and/or Taylor–Görtler vortices can cause the catastrophic breakdown of laminar to turbulent flow, which leads to increased skin-friction drag for the aircraft. The discussion in this Note will be limited to disturbances that evolve along the attachment line (leading edge of swept wing). If the Reynolds number of the attachment-line boundary layer is greater than some critical value, then the complete wing is inevitably engulfed in turbulent flow. Essentially, there are two critical Reynolds number points that must be considered. The first is for small-amplitude disturbances, and the second is for bypass transition.

Summarized in Table 1, the experimental and theoretical results agree for the critical Reynolds number where small-amplitude disturbances become unstable on the attachment line.[1–4] Accounting for all linear terms, and using an eigenvalue problem approach, Hall et al.[5] studied the linear stability of disturbances in the attachment-line boundary-layer flow called swept Hiemenz flow, which is sketched in Fig. 1. By assuming instability modes that were periodic along the attachment line, the calculations by Hall et al.[5] agreed with the experiments and with the direct numerical simulations (DNS) of Spalart,[6] Theofilis,[7] Jiménez et al.,[8] and Joslin.[9,10]

For large-amplitude disturbances, turbulence decays below some critical Reynolds number and transition to turbulence will occur above this point. At this critical point, termed bypass Reynolds number, transition bypasses the conventional linear instability breakdown process. Summarized in Table 2, the experiments show that disturbances are damped for $R_\theta < 1 \times 10^2$ and the flow becomes turbulent for $R_\theta > 1 \times 10^2$ (Refs. 1 and 11–14).

Hall and Malik[15] attempted to explain this discrepancy between linear theory and the turbulent suppression limits by studying the nonlinear disturbances using weakly nonlinear theory and temporal DNS. Subcritical instability was observed in the computations; however, this subcritical growth did not provide the connection between linear instability and the contamination regions.

Note the wide gap between the linear critical Reynolds number of $R_\theta \simeq 2.45 \times 10^2$ and the turbulent suppression critical Reynolds number of $R_\theta \simeq 1 \times 10^2$. Bridging this gap is important for wing design. The present study will use direct numerical simulations to validate a linear two-dimensional eigenvalue prediction method based on parabolized stability equations by Lin and Malik.[16] This method is considered because it suggests that a number of symmetric and asymmetric modes exist and are stable or unstable on the attachment line depending on the Reynolds number. If validated, the approach would predict a number of modes that are linearly damped in the Reynolds number regime 1×10^2 to 2.45×10^2; however, these modes may grow nonlinearly and provide an explanation to this region.

Table 1 Critical Reynolds numbers for attachment-line instabilities

Experiment	Critical R_θ
Cumpsty and Head[1]	2.45×10^2
Pfenninger and Bacon[2]	2.40×10^2
Poll[3,4]	2.30×10^2
Calculations	2.45×10^2

Table 2 Experimental critical points for attachment-line turbulence suppression

Experiment	Bypass R_θ
Pfenninger[11]	1.0×10^2
Gregory and Love[12]	$9.5\text{–}9.8 \times 10^1$
Gaster[13]	$8.8\text{–}10.4 \times 10^1$
Cumpsty and Head[1]	1×10^2
Poll[14]	1×10^2

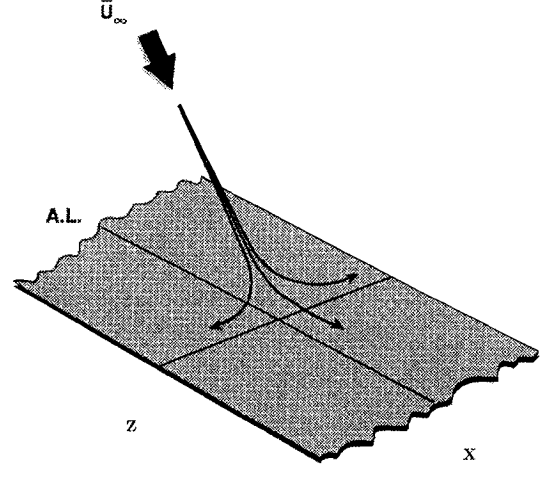

Fig. 1 Sketch of attachment-line region of swept Hiemenz flow.

Received April 8, 1996; revision received July 8, 1996; accepted for publication July 16, 1996; also published in *AIAA Journal on Disc*, Volume 2, Number 1.

*Leader, Laminar Flow Control Project Team, Fluid Mechanics and Acoustics Division. Member AIAA.

Problem Formulation

In general, the velocities $\tilde{\underline{u}} = (\tilde{u}, \tilde{v}, \tilde{w})$ and the pressure $\tilde{p}$ are solutions of the incompressible, unsteady Navier–Stokes equations. The instantaneous velocities $\tilde{\underline{u}}$ and the pressure $\tilde{p}$ may be decomposed into base-flow velocities $\underline{U} = (U, V, W)$ and pressure P and disturbance velocities $\underline{u} = (u, v, w)$ and pressure p. The base flow, originally described by Hall et al.,[5] is referred to as a swept Hiemenz flow. The disturbance is found by solving the three-dimensional incompressible Navier–Stokes equations (in disturbance form)

$$\frac{\partial \underline{u}}{\partial t} + (\underline{u}\cdot\nabla)\underline{u} + (\underline{U}\cdot\nabla)\underline{u} + (\underline{u}\cdot\nabla)\underline{U} = -\nabla p + \frac{1}{R}\nabla^2\underline{u} \qquad (1)$$

$$\nabla\cdot\underline{u} = 0$$

with boundary conditions

$$\underline{u} = 0 \quad \text{at} \quad y = 0 \qquad \text{and} \qquad \underline{u} \to 0 \quad \text{as} \quad y \to \infty \qquad (2)$$

A Cartesian coordinate system $\underline{x} = (x, y, z)$ is used in which x is aligned with the attachment line, y is wall normal, and z corresponds to the direction of flow acceleration away from the attachment line. A boundary-layer thickness is defined in the y–z plane as $\delta = \sqrt{(\nu L/W_0)}$; a Reynolds number, as $R = U_0\delta/\nu$; U_0, V_0, and W_0 are velocity scales; and L is the length scale in the flow-acceleration direction z. If the attachment line is assumed to be infinitely long, the velocities become functions of z and y only, and the similarity solution can be found.

Numerical Method of Solution

The three-dimensional DNS code as described by Joslin[10] is used for the present validation study. High-order finite and central differences are used in the attachment-line (x) direction, and Chebyshev series are used in the wall-normal (y) and flow-acceleration (z) directions. For time marching, a time-splitting procedure was used with implicit Crank–Nicolson differencing for normal diffusion terms; an explicit three-stage Runge–Kutta method was used for the remaining terms.

The disturbances are assumed to be from the discrete spectrum, which exponentially decay with distance from the wall. At the wall, in the far field, and at the flow-acceleration boundaries, homogeneous Dirichlet conditions are imposed. The base flow is used for the inflow boundary condition.

Symmetric and Asymmetric Instability Approach

Recently, Lin and Malik[16,17] have shown with theory that both symmetric and asymmetric instabilities are present in incompressible and compressible swept Hiemenz flow. The solutions posed by Lin and Malik[16] took the form

$$\{u, v, w\}(x, y, z, t) = \{u, v, w\}(y, z)e^{i(\alpha x - \omega t)} \qquad (3)$$

Substituting this form into the Navier–Stokes equations leads to a system of partial differential equations in the flow-acceleration and wall-normal directions. The boundary conditions for the z boundaries took the following form.

Symmetric:

$$\frac{\partial u}{\partial z} = \frac{\partial v}{\partial z} = w = 0 \quad \text{at} \quad z = 0 \qquad (4)$$

$$\{u, v\}(y, z) = \{u, v\}(y, -z), \qquad w(y, z) = -w(y, -z)$$

$$\text{at} \quad z = z_{\max} \qquad (5)$$

Asymmetric:

$$u = v = \frac{\partial w}{\partial z} = 0 \quad \text{at} \quad z = 0 \qquad (6)$$

$$\{u, v\}(y, z) = -\{u, v\}(y, -z), \qquad w(y, z) = w(y, -z)$$

$$\text{at} \quad z = z_{\max} \qquad (7)$$

For the simulations, the entire attachment-line region is included within the computational domain, and therefore the boundary conditions at $z = 0$ are not needed.

The theory suggests that the most unstable modes follow the sequence symmetric (S1), asymmetric (A1), symmetric (S2), etc., where the growth rates of modes are S1 > A1 > S2 > A2 > S3, . . . , without exception. This theory and modal growth ordering were recently confirmed by Fedorov[18] using an asymptotic theory. Although according to the Fedorov analysis, the validation of a single mode implies the validation of all modes, here the first two dominant modes are simulated.

From the results of the Lin–Malik technique,[16] the wave number and growth rate for the first three modes at $R = 7 \times 10^2$ ($R_\theta \simeq 2.82 \times 10^2$) and $\omega = 0.1017$ are shown in Table 3. The simulation of a pure mode will prove difficult because the discrimination of the wave numbers would be difficult. The theoretical results suggest that the previous simulations of discrete modes are, in fact, spectrally rich. To use suction and blowing to generate the S1 mode in the absence of the S2 mode is probably not possible. However, a discriminating factor can be attributed to the phase relation between the symmetric vs asymmetric modes across the attachment line and in the flow-acceleration direction. This difference is obvious from the $z = 0$ boundary conditions (4) and (6). Hence, simulations could discriminate between symmetric and asymmetric modes.

Results

The simulations are performed on a grid of 661 points ($\simeq$ 60 points per wavelength) along the attachment line, 81 points in the wall-normal direction, and 25 points in the flow-acceleration direction. The far-field boundary is located at 40δ from the wall, the computational length along the attachment line is 216δ, and the flow-acceleration boundaries are located $\pm 100\delta$. The total Cray C-90 cost for each simulation is 13 h for 8 periods in time. Separately, the symmetric (S1) and asymmetric (A1) modes were forced using suction and blowing. The phase of the A1 mode in the flow-acceleration direction was determined using the Lin–Malik technique.[16]

In Figs. 2 and 3, the simulation results are compared with the wave growth rates described by the theory (listed in Table 3). The agreement is remarkably good considering the differences between the DNS and assumed solution form (4). For the theory, the A1 mode has a constant wave number and growth rate in the flow-acceleration direction, whereas the simulations have a truly three-dimensional instability, and therefore spectral differences in the z direction are

Table 3 Lin and Malik[16] eigenvalues for swept Hiemenz flow at $R = 7 \times 10^2$ and $\omega = 0.1017$

Mode	α_r	α_i
S1	0.27481152	-0.226959×10^{-2}
A1	0.27515243	-0.105988×10^{-2}
S2	0.27548905	$+0.148157 \times 10^{-3}$

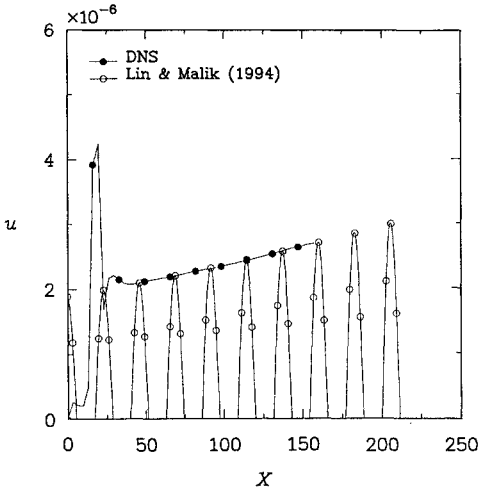

Fig. 2 Symmetric disturbance (S1) growth compared with theory for three-dimensional attachment-line basic flow for $R = 7 \times 10^2$ and $\omega = 0.1017$.

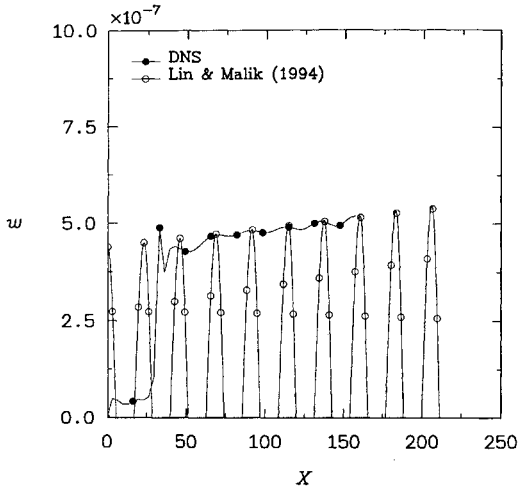

Fig. 3 Asymmetric disturbance (A1) growth compared with theory for three-dimensional attachment-line basic flow for $R = 7 \times 10^2$ and $\omega = 0.1017$.

inevitable in this three-dimensional flow. To make this comparison, the results for the simulation are averaged over the flow-acceleration stations: $z = 0$ and $z = \pm 6$. These stations were selected because, as Joslin[10] shows, the streamlines very near the attachment line are essentially aligned with the two-dimensional attachment-line flow. The $z = \pm 6$ stations permit a cancellation of any opposing flow-acceleration effects.

Concluding Remarks

In this study, results are presented for the spatial DNS of three-dimensional symmetric and asymmetric disturbances that propagate along the attachment line of swept Hiemenz flow. The comparison between the DNS results and the theoretical results demonstrate that both symmetric and asymmetric modes are present in the attachment-line flow and that the theory adequately predicts these modes and the relative dominance of each mode.

Although the connection between the linear instability $R_\theta \simeq 2.45 \times 10^2$ and the turbulent contamination $R_\theta \simeq 1 \times 10^2$ regions was not definitively explained, it is clear that a wealth of instabilities can be present within this three-dimensional flowfield and that some combination of these modes interacting in a nonlinear manner will likely resolve this region of study.

Acknowledgment

The author wishes to express his gratitude to R.-S. Lin, High Technology Corporation, for providing the initial disturbance information for the simulations.

References

[1]Cumpsty, N. A., and Head, M. R., "The Calculation of the Three-Dimensional Turbulent Boundary Layer. Part III. Comparison of Attachment-Line Calculations with Experiment," *Aeronautical Quarterly*, Vol. 20, May 1969, pp. 99–113.

[2]Pfenninger, W., and Bacon, J. W., Jr., "Amplified Laminar Boundary-Layer Oscillations and Transition at the Front Attachment Line of a 45 Degree Swept Flat-Nosed Wing With and Without Boundary-Layer Suction," *Viscous Drag Reduction*, edited by C. S. Wells, Plenum, New York, 1969, pp. 85–105.

[3]Poll, D. I. A., "Transition in the Infinite Swept Attachment Line Boundary Layer," *Aeronautical Quarterly*, Vol. 30, Nov. 1979, pp. 607–628.

[4]Poll, D. I. A., "Three-Dimensional Boundary Layer Transition via the Mechanisms of Attachment-Line Contamination and Crossflow Stability," *Laminar-Turbulent Transition*, edited by R. Eppler and H. Fasel, Springer, Stuttgart, Germany, 1980, pp. 253–262.

[5]Hall, P., Malik, M. R., and Poll, D. I. A., "On the Stability of an Infinite Swept Attachment Line Boundary Layer," *Proceedings of the Royal Society of London, Series A: Mathematical and Physical Science*, Vol. 395, Oct. 1984, pp. 229–245.

[6]Spalart, P. R., "Direct Numerical Study of Leading-Edge Contamination," AGARD, CP-438, 1989, pp. 5.1–5.13.

[7]Theofilis, V., "Numerical Experiments on the Stability of Leading Edge Boundary Layer Flow: A Two-Dimensional Linear Study," *International Journal for Numerical Methods in Fluids*, Vol. 16, Jan. 1993, pp. 153–170.

[8]Jiménez, J., Martel, C., Agüí, J. C., and Zufiria, J. A., "Direct Numerical Simulation of Transition in the Incompressible Leading Edge Boundary Layer," *ETSIA/MF-903*, Universidad Politecnica Madrid, Spain, 1990.

[9]Joslin, R. D., "Direct Simulation of Evolution and Control of Nonlinear Instabilities in Attachment-Line Boundary Layers," AIAA Paper 94-0826, Jan. 1994.

[10]Joslin, R. D., "Direct Simulation of Evolution and Control of Three-Dimensional Instabilities in Attachment-Line Boundary Layers," *Journal of Fluid Mechanics*, Vol. 291, May 1995, pp. 369–392.

[11]Pfenninger, W., "Flow Phenomena at the Leading Edge of Swept Wings," *Recent Developments in Boundary Layer Research*, AGARD 97, May 1965.

[12]Gregory, N., and Love, E. M., "Laminar Flow on a Swept Leading Edge," National Physical Lab., Final Progress Rept., NPL Aero. Memo., Vol. 26, Oct. 1965.

[13]Gaster, M., "On the Flow Along Swept Leading Edges," *Aeronautical Quarterly*, Vol. 18, May 1967, pp. 165–184.

[14]Poll, D. I. A., "Some Observations of the Transition Process on the Windward Face of a Long Yawed Cylinder," *Journal of Fluid Mechanics*, Vol. 150, Jan. 1985, pp. 329–356.

[15]Hall, P., and Malik, M. R., "On the Instability of a Three-Dimensional Attachment-Line Boundary Layer: Weakly Nonlinear Theory and a Numerical Simulation," *Journal of Fluid Mechanics*, Vol. 163, Feb. 1986, pp. 257–282.

[16]Lin, R.-S., and Malik, M. R., "The Stability of Incompressible Attachment-Line Boundary Layers—A 2D-Eigenvalue Approach," AIAA Paper 94-2372, June 1994.

[17]Lin, R.-S., and Malik, M. R., "Stability and Transition in Compressible Attachment-Line Boundary-Layer Flow," Aerotech '95, Society of Automotive Engineers, SAE Paper 952041, Los Angeles, CA, Sept. 1995.

[18]Fedorov, S., personal communication, Moscow Inst. of Physics and Technology, Zhukovsky, Russia, 1995.

Transition Detection with Deposited Hot Films in Cryogenic Tunnels

Ehud Gartenberg*
Old Dominion University, Norfolk, Virginia 23529-0247
and
Michael A. Scott† and Scott D. Martinson‡
NASA Langley Research Center, Hampton, Virginia 23681-0001

Introduction

CRYOGENIC wind tunnels are high Reynolds number facilities, capable of producing on models the Mach–Reynolds numbers combinations occurring on large transport airplanes in flight. These are subsonic and transonic tunnels in which liquid nitrogen is continuously injected into the stream and gas is vented to keep the pressure and temperature values at the desired test condition. The temperature can be varied between ambient and 120 K, while the pressure can be varied according to the tunnel's design. Under typical test conditions, the unit Reynolds number is 30 to 40 times higher than in flight, and about 4 times higher than in conventional tunnels operating at identical pressures. The capability to detect boundary-layer

Received June 30, 1995; revision received July 16, 1996; accepted for publication July 22, 1996; also published in *AIAA Journal on Disc*, Volume 2, Number 1.

*Research Associate Professor, Department of Mechanical Engineering. Associate Fellow AIAA.
†Aerospace Technologist, Aerodynamic Measurement Branch, MS 234.
‡Aerospace Technologist, Acoustical, Optical, and Chemical Measurement Branch, MS 236.